

UNCLASSIFIED

AD NUMBER

AD825414

LIMITATION CHANGES

TO:

Approved for public release; distribution is unlimited.

FROM:

Distribution: Further dissemination only as directed by Army Electronics Command, Fort Monmouth, NJ 07703, DEC 1967, or higher DoD authority.

AUTHORITY

usaec ltr, 16 jun 1971

THIS PAGE IS UNCLASSIFIED



RESEARCH AND DEVELOPMENT TECHNICAL REPORT

ECOM-01821-7

# INVESTIGATION OF HIGH-POWER BEAM PLASMA INTERACTIONS

7TH QUARTERLY REPORT

BY

DAVID MORSE

HARRY EWALD

CLAUDE LUSTIG

DECEMBER 1967

DISTRIBUTION STATEMENT  
 This document is not to be distributed outside  
 the Department of Defense without prior  
 approval of the U.S. Army Electronics  
 Command, Fort Monmouth, N.J.  
 Attn: AMSBL-KL-TG

D D C  
 RECEIVED  
 JAN 3 1968  
 RESERVE  
 B

# ECOM

UNITED STATES ARMY ELECTRONICS COMMAND • FORT MONMOUTH, N.J. 07703

Sponsored By Advanced Research Projects Agency Under Project Defender

CONTRACT DA 28-043-AMC-01821(E), ARPA Order No. 695

 **SPERRY RAND** RESEARCH CENTER  
 SUDBURY, MASSACHUSETTS 01776

AD825414

## NOTICES

### Disclaimers

The findings in this report are not to be construed as an official Department of the Army position, unless so designated by other authorized documents.

The citation of trade names and names of manufacturers in this report is not to be construed as official Government indorsement or approval of commercial products or services referenced herein.

### Disposition

Destroy this report when it is no longer needed. Do not return it to the originator.

INVESTIGATIONS OF HIGH-POWER  
BEAM PLASMA INTERACTIONS

7th QUARTERLY REPORT  
15 June 1967 - 14 September 1967  
Report No. 7  
Contract No. DA 28-043-AMC-01821(E)  
DA Project No. 7900.21.243.40.01

Prepared By  
David Morse, Harry Ewald and Claude Lustig  
Sperry Rand Research Center

for  
U. S. Army Electronics Command, Fort Monmouth, N. J. 07703

Sponsored By  
Advanced Research Projects Agency  
ARPA Order No. 695

This research is part of PROJECT DEFENDER, sponsored by the Advanced Research Projects Agency, Department of Defense, and administered by the U. S. Army Electronics Command, under Contract No. DA 28-043-AMC-01821(E).

DISTRIBUTION STATEMENT

This document may be further distributed by any holder only with specific prior approval of CG, U. S. Army Electronics Command, Fort Monmouth, N. J. Attn: AMSEL-KL-TG

 **SPERRY RAND** RESEARCH CENTER  
SUDBURY, MASSACHUSETTS 01776

## ABSTRACT

This research is directed toward the investigation of high-power beam plasma interactions, with specific investigation of the transverse velocity beam modes called for.

A system for measuring the transverse energy of an electron beam through its diamagnetism has been developed and used to measure the transverse energy of a beam injected across magnetic field lines. In investigations of the noise emission from a transverse energy beam, discrete noise peaks, which shifted toward higher frequencies when a neutral gas was allowed to enter the vacuum chamber, occurred at the electron-cyclotron frequency and its first three harmonics. Experiments in helium indicate that the emission may be described by a hybrid frequency relationship. Analysis of the data from beam plasma interaction experiments has indicated the possible existence of a transverse energy beam mode on our experiments.

This research is part of PROJECT DEFENDER, sponsored by the Advanced Research Project Agency, Department of Defense, and administered by the U. S. Army Electronics Command under Contract No. DA 28-043-AMC-01821(E).

## TABLE OF CONTENTS

| <u>Section</u> |   | <u>Page</u> |
|----------------|---|-------------|
| I              | PURPOSE   | 1           |
| II             | INTRODUCTION AND STATEMENT OF PROBLEM                 | 1           |
| III            | TECHNICAL BACKGROUND                                  | 2           |
|                | A. Linear Theory of Waves in a Uniform Plasma or Beam | 2           |
|                | B. The Effect of Gradients                            | 7           |
| IV             | WORK PERFORMED DURING REPORT PERIOD                   | 17          |
|                | A. Diamagnetic Measurements                           | 17          |
|                | B. Noise Emission from a Transverse Energy Beam       | 19          |
|                | C. Modulated-Beam Experiment                          | 26          |
| V              | CONCLUSIONS   | 29          |
| VI             | FUTURE PLANS  | 29          |
|                | LITERATURE CITED                                      | 31          |

## LIST OF ILLUSTRATIONS

| <u>Figure</u> |   | <u>Page</u> |
|---------------|---|-------------|
| 1             | Dispersion diagram of so-called electron beam where electrons move only along the magnetic field with a single speed (in this case zero velocity).  | 4           |
| 2             | Dispersion diagram for transverse beam modes on a mono-energetic beam of spiraling electrons.   | 5           |
| 3             | Dispersion relation for mono-energetic, fixed perpendicular energy beam waves of frequency less than the first cyclotron harmonic.  | 8           |
| 4             | Growth rate and frequency of growing waves associated with the interaction of the positive energy beam wave with the negative energy beam wave on the same beam as a function of the ratio of cyclotron to beam plasma frequency. | 9           |
| 5             | Reactive interaction between a transverse velocity beam and a warm plasma.  | 10          |
| 6             | Electric potential associated with the radial wave resonances on a plasma column.   | 13          |
| 7             | Experimentally observed radial electron plasma wave resonances in the core of a cylindrical plasma column for different magnetic field strengths.   | 15          |
| 8             | Experimental apparatus showing method of excitation as well as method of internal probing of radial resonances on a plasma column in magnetic field.  | 16          |
| 9             | Experimental arrangement for measuring diamagnetism of electron beam.   | 20          |
| 10            | Variation of diamagnetic flux with beam current for different magnetic fields with a fixed beam energy.   | 21          |
| 11            | Percentage of final beam energy in the transverse plane as a function of axial magnetic field.  | 22          |
| 12            | Variation of diamagnetic flux with beam current for different beam currents at a fixed magnetic field.  | 23          |
| 13            | Percentage of final beam energy in the transverse plane as a function of the total energy in the electron beam.   | 24          |

# LIST OF ILLUSTRATIONS (cont.)

| <u>Figure</u> |   | <u>Page</u> |
|---------------|---|-------------|
| 14            | Percentage of final beam energy in the transverse plane as a function of the axial position of the gun. | 25          |
| 15            | Dependence of noise frequency radiated by transverse energy beam on axial magnetic field.               | 27          |
| 16            | Frequency of noise emitted near the cyclotron frequency as a function of helium pressure.               | 28          |
| 17            | Axial beam voltage $V$ at which maxima, numbered $n$ , are observed with a fixed probe in the plasma.   | 30          |



## I. PURPOSE

This investigation has as its purpose the theoretical and experimental investigation of new (i.e., not space charge) modes of beam plasma interaction. In particular, it includes the investigation of the feasibility of these new modes as an improved means of generation and amplification of microwaves.

## II. INTRODUCTION AND STATEMENT OF PROBLEM

It is apparent from recent developments in the linear theory of plasma waves (of which electron beam waves are a subgroup) that the wave interactions used thus far in devices for microwave generation and amplification represent only a small fraction of those which are possible and which should be considered. Performance and design limitations of existing devices are due to the characteristics of the particular waves used, and they may well be extended or removed if different waves are employed.

The Sperry Rand Research Center (SRRC) has contracted to conduct a comprehensive theoretical and experimental study of particular plasma waves (including electron beam waves) which are candidates for application to high-power microwave generators or amplifiers and which have not as yet been adequately investigated.

The work being undertaken is an extension of research which has been in progress at SRRC. As a result of company sponsored investigations performed during the past three years, an important set of beam and plasma waves - the so-called electrostatic, cyclotron-harmonic waves - have been identified. These waves merit further study because they remove the plasma density, magnetic field, and parallel phase velocity restrictions inherent in the wave modes used in existing devices. Their dispersion relation has been formulated and solved for many interesting cases, including growing wave interactions.

In particular the research program includes measurement of propagation characteristics for comparison with existing linear dispersion theory; coordinated theoretical and experimental study of the effect of finite geometry, velocity spread, and density and temperature gradients on linear propagation characteristics and wave impedance; a primarily experimental study of nonlinear amplitude limiting and spurious frequency generation; and a study of the noise properties of the amplification medium. Special emphasis will be given to a search for practical methods of efficiently coupling these waves to conventional transmission lines.

The program will also include extension of the range of solutions to linear plasma and beam wave dispersion relations in a search for additional wave modes of potential usefulness in high-power microwave devices. For while the past theoretical program at SRRC has been extensive, there remain many possible relative orientations of beam velocity, wave velocity, rf electric field and dc magnetic field vectors, wide ranges of parameters, and many beam and plasma velocity distributions of potential interest which have not yet been considered.

### III. TECHNICAL BACKGROUND

#### A. LINEAR THEORY OF WAVES IN A UNIFORM PLASMA OR BEAM

The non-relativistic dispersion relation for high-frequency electrostatic waves in an infinite uniform electron medium neutralized by massive ions is:

$$\frac{\omega_p^2}{k_\perp^2 + k_\parallel^2} \sum_{n=-\infty}^{\infty} \int_0^\infty v_\perp dv_\perp \int_{-\infty}^{\infty} dv_\parallel \frac{2\pi J_n^2(k_\perp v_\perp / \Omega)}{\omega - k_\parallel v_\parallel - n\Omega} \left( \frac{n\Omega}{v_\perp} \frac{\partial}{\partial v_\perp} + k_\parallel \frac{\partial}{\partial v_\parallel} \right) f_0(v_\perp, v_\parallel) = -1 \quad (1)$$

where

$$\omega_p^2 = \frac{ne^2}{\epsilon_0 m}$$

$k_\parallel$  = component of propagation vector along the static magnetic field,  $B_0$ .

$k_\perp$  = component of propagation vector across the static magnetic field.

$f_0(v_\perp, v_\parallel)$  = the normalized electron velocity distribution where  $v_\perp$  is the velocity across the field and  $v_\parallel$  is the velocity along the field.

$$\Omega = \frac{eB_0}{m}$$

and  $J_n(k_\perp v_\perp / \Omega)$  is the Bessel function of the first kind and order  $n$  with argument  $k_\perp v_\perp / \Omega$ .

The importance of the distribution function in determining the behavior of the waves which may be supported in the medium is striking. To begin with, if we consider an electron beam with velocity parallel to the magnetic field, then

$$f_0(v_\perp, v_\parallel) = \frac{1}{2\pi v_\perp} \delta(v_\perp) \delta(v_\parallel - v_{0\parallel})$$

and the dispersion relation is

$$k_{\perp}^2 \frac{v_p^2}{(\omega - k_{\parallel} v_{0\parallel})^2} + k_{\parallel}^2 \frac{v_p^2}{(\omega - k_{\parallel} v_{0\parallel})^2 - \Omega^2} = k_{\perp}^2 + k_{\parallel}^2 \quad (2)$$

This equation, originally discussed by Gould and Trivelpiece,<sup>1</sup> describes the fast and slow space charge waves as well as the fast and slow fundamental cyclotron waves. The case of a finite beam diameter has also been discussed in detail.<sup>2</sup> The general conclusion drawn from the simple case of a uniform density finite diameter beam is that the geometry merely restricts the set of  $k$  values ( $k_{\perp}, k_{\parallel}$ ) which can be used to satisfy (2) but that the infinite medium dispersion equation must still be satisfied. The dispersion diagram for this "cold" electron beam is given in Fig. 1. It will be noted that the slow "negative energy" waves used for oscillators or amplifiers have a parallel phase velocity less than the beam velocity.

When electron motion about the lines of magnetic field is taken into account, an infinite set of waves is found.<sup>3,4</sup> In addition to modified space charge waves, two waves exist for each harmonic of the electron cyclotron frequency. One of each such pair of waves is found to have negative energy,<sup>5</sup> and can thus be used for growing wave interaction, as is the slow space charge wave in conventional microwave tubes. The dispersion curve shown in Fig. 2 is for a beam of monoenergetic, spiraling electrons, whose velocity distribution is given by

$$f_0(v_{\perp}, v_{\parallel}) = \frac{1}{2\pi v_{0\perp}} \delta(v_{\perp} - v_{0\perp}) \delta(v_{\parallel} - v_{0\parallel})$$

and whose dispersion relation is

$$k^2 = k_{\perp}^2 + k_{\parallel}^2 = \frac{v_p^2}{\omega} \sum_{n=-\infty}^{\infty} \left[ \frac{k_{\perp}^2 J_n^2(k_{\perp} v_{0\perp} / \Omega)}{(\omega - k_{\parallel} v_{0\parallel} - n\Omega)^2} + \frac{k_{\parallel}^2 [J_{n-1}^2(k_{\perp} v_{0\perp} / \Omega) - J_{n+1}^2(k_{\perp} v_{0\perp} / \Omega)]}{2(\omega - k_{\parallel} v_{0\parallel} - n\Omega)} \right] \quad (3)$$

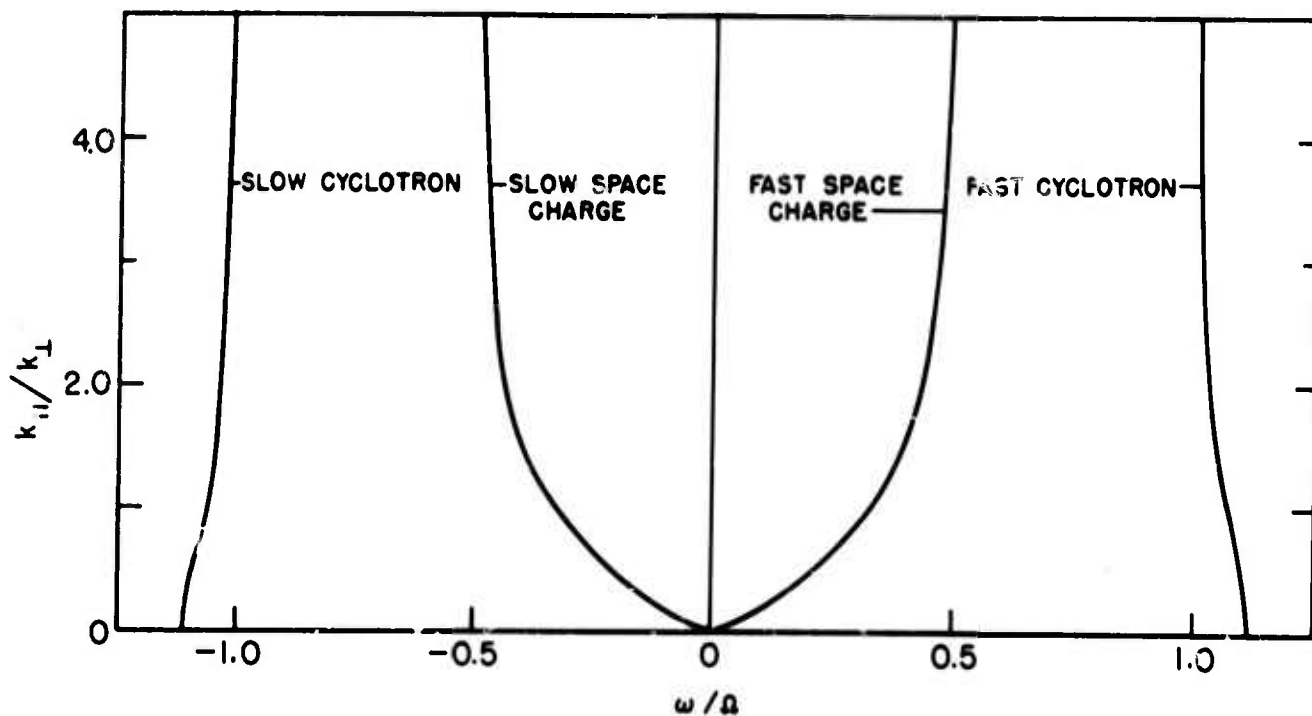


FIG. 1 Dispersion diagram of so-called cold electron beam where electrons move only along the magnetic field with a single speed (in this case zero velocity). The beam plasma frequency divided by the cyclotron frequency  $\omega_p/\Omega = 0.5$  for the example chosen.

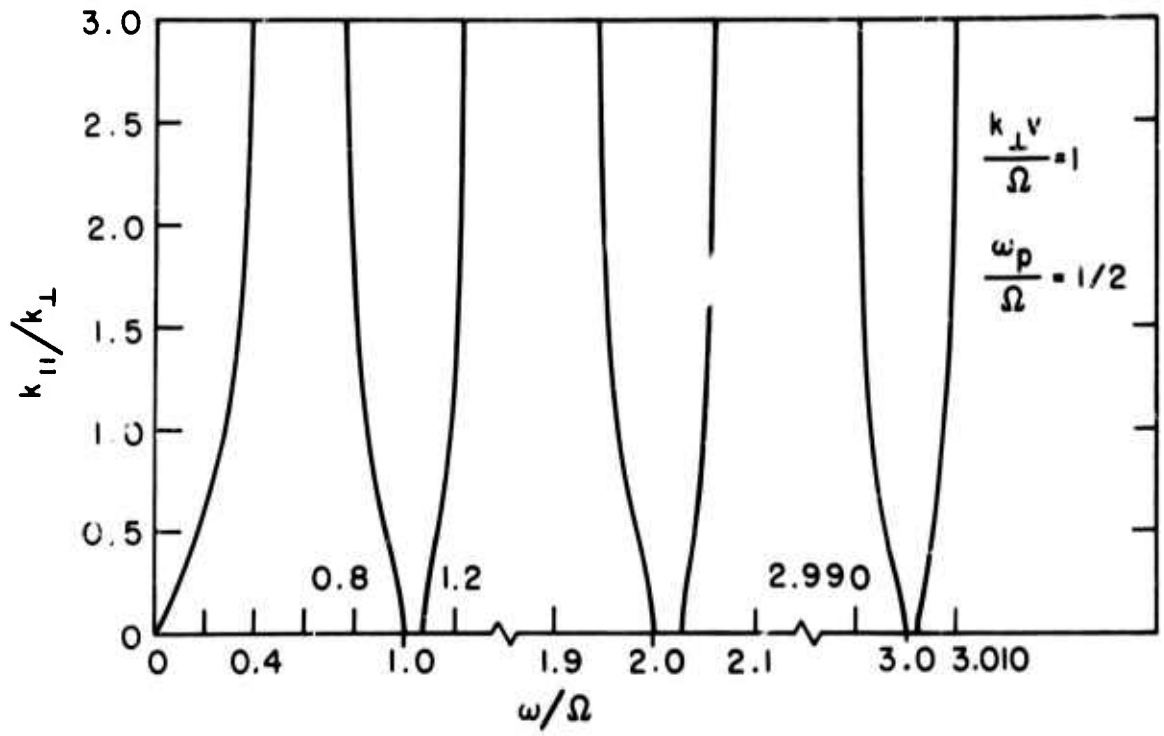


FIG. 2 Dispersion diagram for transverse beam modes on a mono-energetic beam of spiraling electrons. Only positive frequencies are shown for convenience. The dispersion relation is symmetric about both axes. Here again  $\omega_p/\Omega = 0.5$  but  $v_{0\perp} = \Omega/k_{\perp}$  (fixed  $k_{\perp}$ ).

If we consider an electron beam whose distribution function is Maxwellian across the field and having a single velocity along the field, then the results of using this in Eq. (1) yields

$$k^2 = k_{\perp}^2 + k_{\parallel}^2 = \omega_p^2 \sum_{n=-\infty}^{\infty} I_n(\lambda) e^{-\lambda} \left[ \frac{k_{\parallel}^2 v_{\perp}^2}{(\omega - k_{\parallel} v_{0\parallel} - n\Omega)^2} + \frac{n\Omega}{(\omega - k_{\parallel} v_{0\parallel} - n\Omega)} \right] \quad (4)$$

where

$$\lambda = (k_{\perp} v_{\perp} / \Omega)^2 .$$

Equation (3) exhibits certain interesting characteristics which in principle may be utilized in a power generation system. Consider the function in the last sum on the right-hand side of the equation,

$$J_{n-1}^2(\rho) - J_{n+1}^2(\rho) = J_n(\rho) \frac{d}{d\rho} J_n(\rho) .$$

where

$$\rho = k_{\perp} v_{0\perp} / \Omega .$$

This function becomes negative whenever  $J_n(\rho)$  and its derivative are of opposite sign. It is possible, for a sufficiently dense beam, to have instability over critical perpendicular velocity ranges for which  $J_n(\rho) d/d\rho J_n(\rho)$  is negative. Too much velocity spread in the perpendicular direction can eliminate these unstable regions, however, since the Maxwellian velocity distribution beam does not exhibit this characteristic. Our theoretical investigation will include detailed calculations of the effect both of perpendicular velocity spread (we will employ a shifted Maxwellian distribution with variable velocity spread) and of axial velocity spread, a spread which leads to the so-called "collisionless cyclotron damping."

Interaction between the transverse velocity, negative energy wave on the beam near the cyclotron harmonic and a circuit (or beam or plasma) positive energy wave leads to wave growth. This is dramatically illustrated in Fig. 3, where we present the negative and positive energy waves on a single electron beam. As the beam electron density increases, the positive energy wave originating at zero frequency for  $k_{\parallel} = 0$  (the fast space charge wave) couples with the negative-energy transverse velocity wave at the cyclotron frequency, and an instability results in growing wave solutions.<sup>6</sup> The growth rate and frequency spectrum of these waves are presented in Fig. 4 for several harmonics of the electron cyclotron frequency.

The interaction of a monoenergetic beam excited in the transverse velocity mode with a plasma whose electrons have a Maxwellian velocity distribution has been considered under somewhat restricted conditions by us. We have found wave growth in the region where the axially-traveling beam electrons see the cyclotron harmonic frequencies after the approximate doppler shift. This interaction occurs if the plasma appears to be lossy (resistive instability) or slightly reactive (reactive instability). In Fig. 5 we show the results of a calculation of the reactive instability.

The effect of boundaries in a finite beam of uniform electron density is subtly complicated by the non-zero orbits of the electrons. Those electrons traveling on field lines within a Larmor radius of the outer edge of the beam penetrate through the beam boundary and, hence, through what would be a region of radial field discontinuity. These electrons may interact more strongly with harmonics of the cyclotron motion than electrons nearer the axis.<sup>7</sup>

## B. THE EFFECT OF GRADIENTS

The importance of density and temperature gradients in beams or plasmas is well recognized. Because of theoretical difficulties, few attempts toward adequate solutions have been made. Recently, Nickel, Parker and Gould<sup>8</sup> and others investigated the effect of plasma gradients upon electrostatic waves propagating across a plasma column in order to explain the so-called Tonks-Dattner resonances which occur with no magnetic field. Buchsbaum and Hasegawa<sup>9</sup> and Schmitt, Meltz and Freyheit<sup>10</sup> have considered wave propagation across a radial density gradient in a magnetized plasma. In all cases, it is assumed that the change in density across a Larmor orbit is either so small that the gradient slightly perturbs the wave-equation or so large that the zero magnetic field condition is valid.

Emission<sup>11</sup> and absorption<sup>9,10</sup> measurements of a plasma column immersed in a magnetic field have shown very interesting fine structure when the frequency of observation is in the vicinity of twice the electron cyclotron frequency (and higher harmonics as well). The theory of Buchsbaum and Hasegawa is that waves can propagate within the high-density core of the plasma out toward the walls of the discharge tube until the wave frequency corresponds to the local hybrid frequency ( $\omega_{\text{hybrid}} = \sqrt{\omega_p^2 + \Omega_p^2}$ ), as long as the wave frequency is less than the second harmonic of the cyclotron frequency.

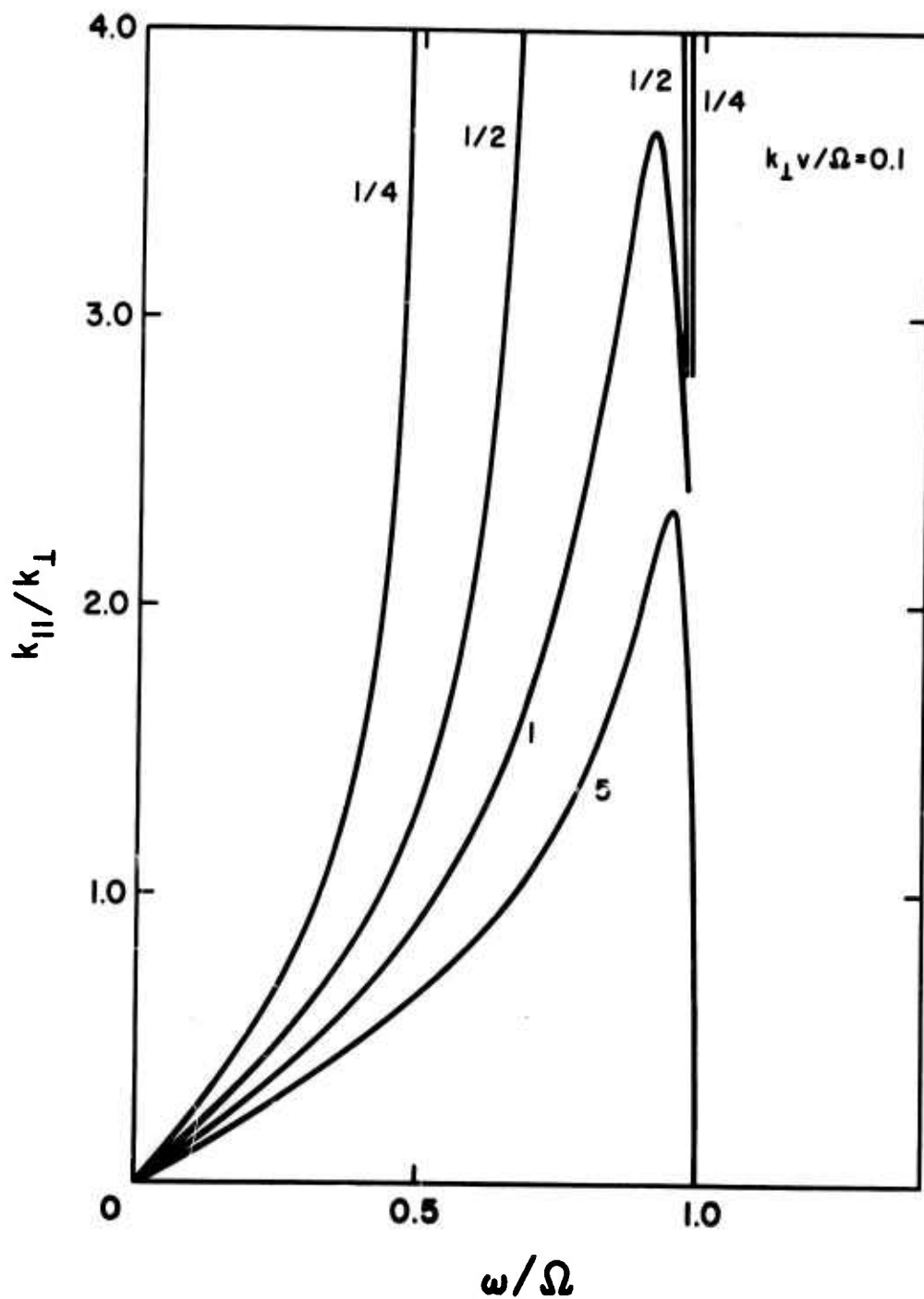


FIG. 3 Dispersion relation for mono-energetic, fixed perpendicular energy beam waves of frequency less than the first cyclotron harmonic. Each curve is for different beam density expressed in terms of the ratio  $\omega_p/\Omega^2$  all having  $k_{\perp}v_{0\perp} = 0.1\Omega$ . As density increases, the wave originating near zero frequency couples with the negative energy wave below the cyclotron frequency, and wave growth ensues.



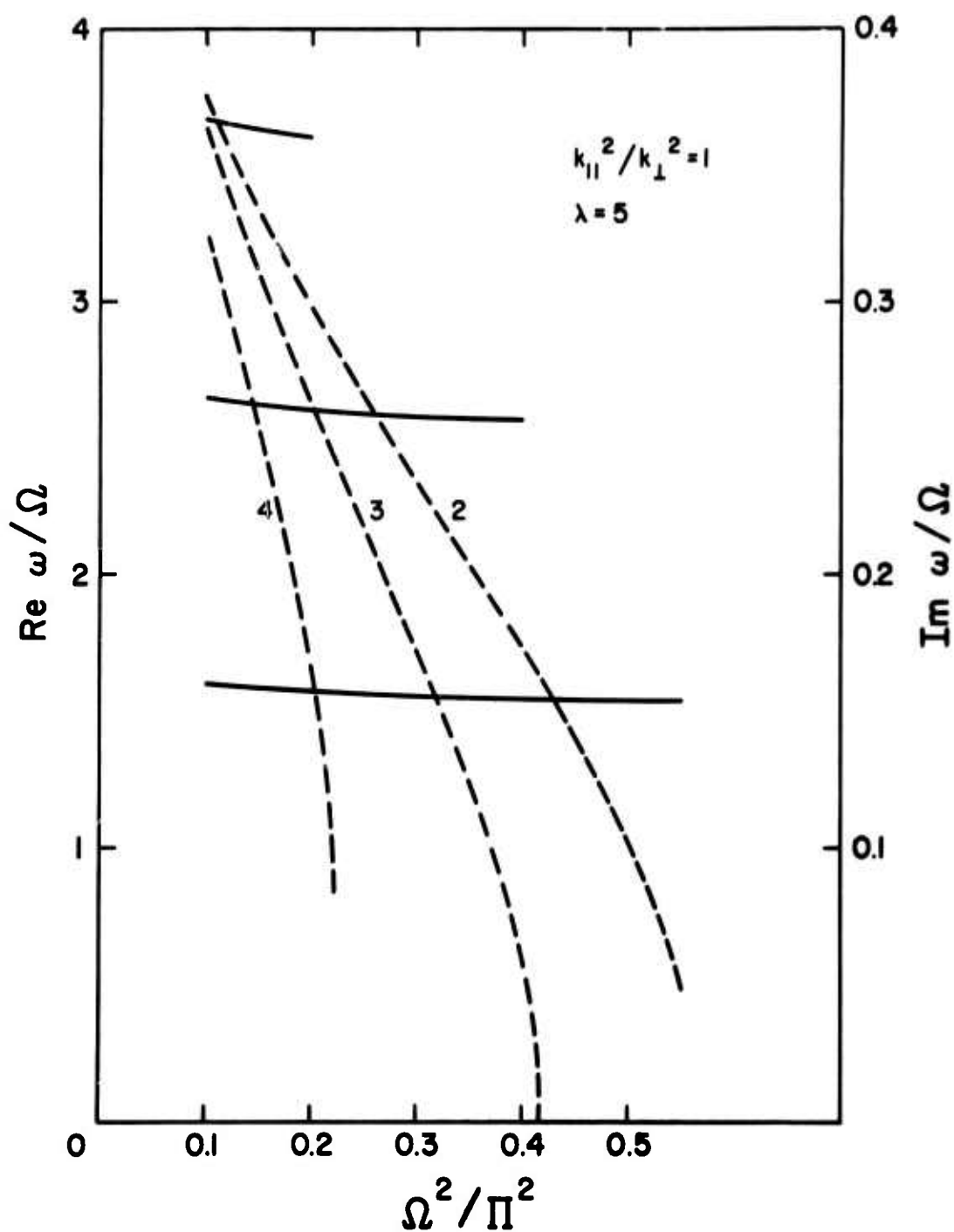


FIG. 4 Growth rate and frequency of growing waves associated with the interaction of the positive energy beam wave with the negative energy beam wave on the same beam as a function of the ratio of cyclotron to beam plasma frequency. Growth curves are shown by the dashed lines.

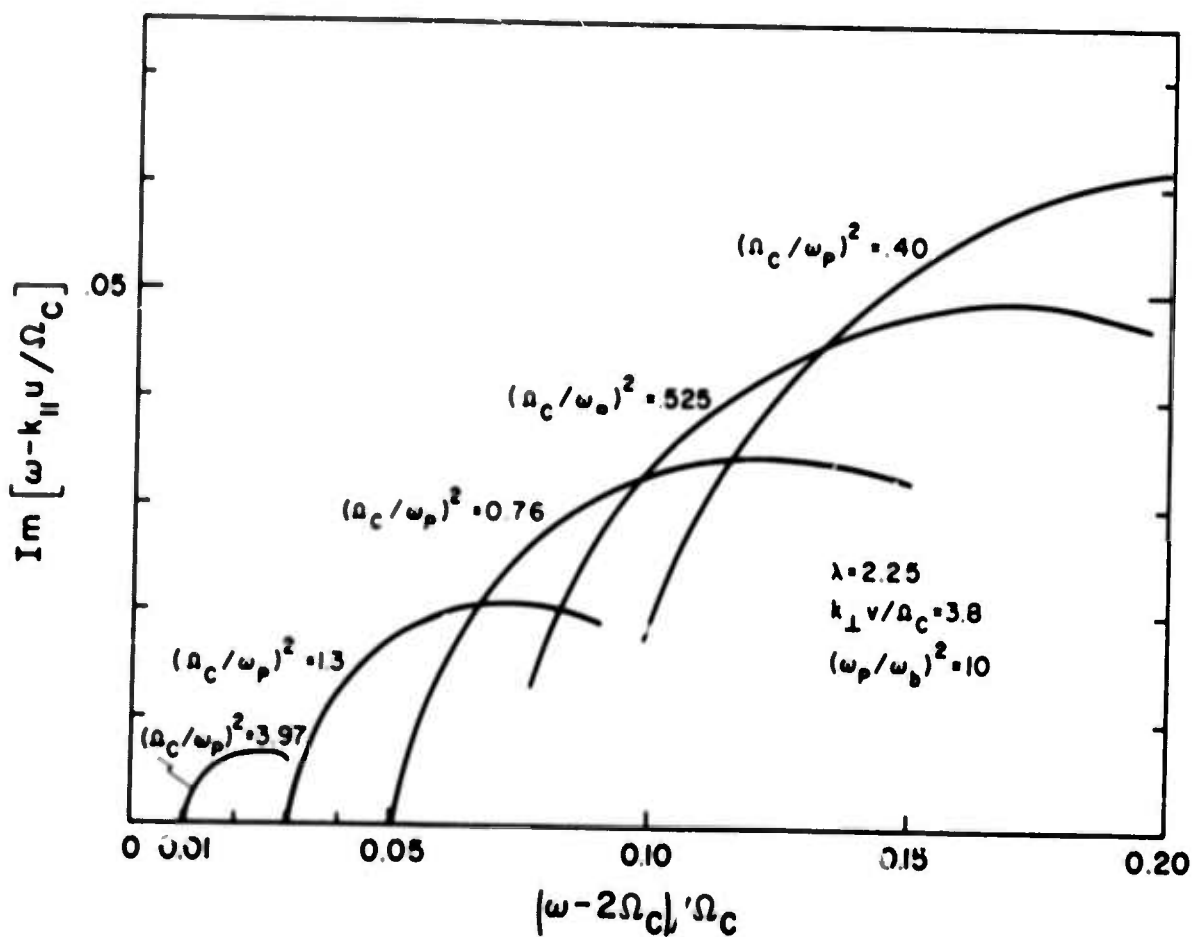


FIG. 5 Reactive interaction between a transverse velocity beam and a warm-plasma. Growth rate vs frequency is presented for waves near the second harmonic of the electron cyclotron frequency. Each curve represents a different plasma electron density, thus showing growth rate and frequency depend upon plasma frequency.

At the hybrid frequency the waves become evanescent on the outside and are reflected toward the interior, thus setting up a standing wave or radial resonant condition. The importance of radial density gradients is stressed by their analysis.

The combination of the linearized Boltzmann equation with Poisson's equation leads to the following differential equation for slab geometry:

$$\frac{d^2}{dx^2} [g(x)E(x)] + \frac{1}{\lambda^2} \left[ \frac{\omega_{po}^2}{\omega^2 - \Omega^2} - \frac{1}{g(x)} \right] g(x)E(x) = 0 \quad (5)$$

where

$$\lambda^2 = \frac{3eT/m \omega_{po}^2}{(\omega^2 - \Omega^2)(4\Omega^2 - \omega^2)} .$$

T is the electron temperature (assumed to be uniform), g(x) is the normalized electron density profile, and  $\omega_{po}$  is the peak electron plasma frequency.

If the medium is uniform,  $g = 1$  and  $d^2/dx^2 \rightarrow -k^2$ , so that the dispersion relation is

$$(4\Omega^2 - \omega^2)(\Omega^2 + \omega_{po}^2 - \omega^2) = k_{\perp}^2 \left( \frac{3eT}{m} \right) \omega_{po}^2 \quad (6)$$

from which we can verify that

k is real where  $\omega^2 < \Omega^2 + \omega_{po}^2$  and  $2\Omega > \omega$  .

k is real where  $\omega^2 > \omega_{po}^2 + \Omega^2$  and  $2\Omega < \omega$  .

Case 2 has been experimentally and theoretically treated by Schmitt, Meltz and Freyheit.<sup>10</sup>

The solution of Eq. (5) can be explicitly given for a density profile

$$g(x) = \frac{1}{1 + \gamma \left(\frac{x}{l}\right)^2}$$

and is

$$E(x) = \left[ 1 + \gamma \left(\frac{x}{l}\right)^2 \right] \left[ D_\nu \left(\frac{x}{c}\right) \pm D_\nu \left(\frac{-x}{c}\right) \right]$$

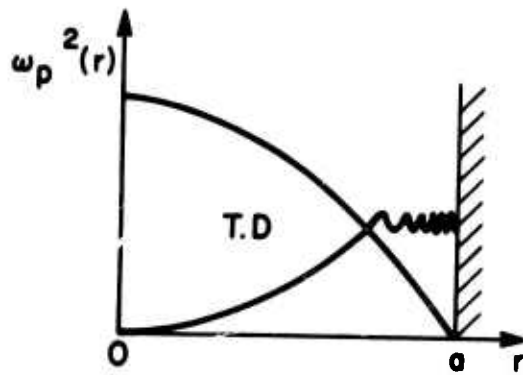
where

$$c = \left[ \frac{\frac{3eT}{m} \omega_{po}^2 l^2}{4\gamma(\omega^2 - \Omega^2)(4\Omega^2 - \omega^2)} \right]^{1/4}$$

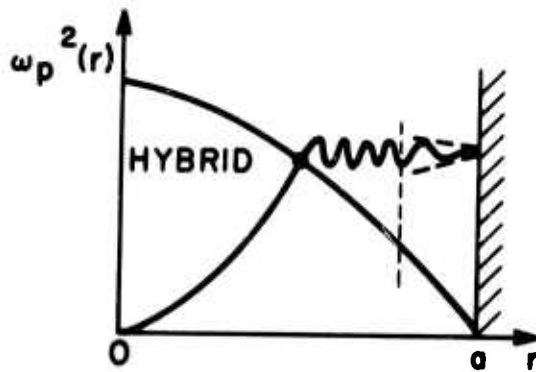
$$\nu = \frac{1}{2} \left[ \left\{ \frac{(4\Omega^2 - \omega^2) l^2}{3\omega_{po}^2 \frac{eT}{m} (\omega^2 - \Omega^2)} \right\}^{1/2} (\Omega^2 + \omega_{po}^2 - \omega^2) - 1 \right]$$

and the  $D$  functions are parabolic cylinder functions. These functions oscillate in space in the manner of a radial standing wave, showing that physically the wave propagating out from the core is continuously reflected from the density gradient. Buchsbaum and Hasegawa's work has been extended by us to include cylindrical geometry, and the same essential feature of the standing wave pattern is found. In Fig. 6 we illustrate the nature of the solutions associated with waves propagating across a density gradient both with and without a static axial magnetic field.

The solution given above for the non-uniform plasma is valid only in the region where  $\omega \approx 2\Omega$  and is a result of an expansion to first order in the quantity  $(L_r d/dx)$ , which is the ratio of Larmor orbit  $(L_r^2 = eT/m\Omega^2)$  to gradient scale length. In order to consider waves in the

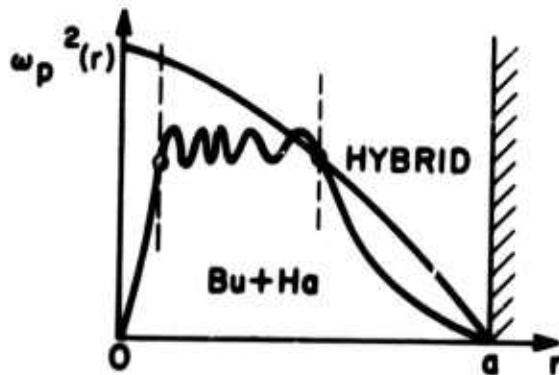


$$\Omega = 0$$



$$p < \frac{\epsilon}{2} < p+1$$

$$(p \geq 2)$$



$$\frac{\epsilon}{2} > 1$$

FIG. 6 Electric potential associated with the radial wave resonances on a plasma column. Three cases are indicated: Tonks-Dattner (TD) resonances with no magnetic field, the Buchsbaum-Hasegawa core resonances (B-H) in a magnetic field and external resonances in a magnetic field.

vicinity of the third harmonic, terms to second order in  $L_r d/dx$  are required and so on. It is obvious that computational complications increase with higher harmonic number if such a technique is used. We propose to consider the extension of this method as well as attempting different attacks on the problem.

While a plasma will probably have only slightly non-uniform electron temperature, an electron beam may well have a velocity distribution (it would be incorrect to consider it a temperature) which is highly inhomogeneous as a result of generation and injection methods. The terms arising from inhomogeneous beam electron velocity distribution (and density gradients) in the Boltzmann equation are from the term  $v_0 \nabla_r f_0$ , where  $f_0 = n(r)g_{\perp}(r, v_{\perp})g_{\parallel}(r, v_{\parallel})$ . That is, we assume that the density and velocity variations are separable. For example, we could consider a local Maxwellian velocity distribution in the  $\perp$  direction.

$$g_{\perp}(r, v_{\perp}) = \frac{1}{\sqrt{2\pi v_{\perp 0}^2(r)}} \exp \left( -\frac{v_{\perp}^2}{2v_{\perp 0}^2(r)} \right).$$

The consequences of such a distribution (or, for that matter, of any temperature gradient) upon the cyclotron harmonic beam waves are not evident, but approaching the problem via a perturbation technique allows the insights obtained in the uniform analysis to be extended and applied to the very difficult case of spatial temperature variation. That is, we can consider

$$v_{\perp 0}^2(r) = v_{\perp 0}^2 \left[ 1 + \gamma \left( \frac{r}{\ell} \right)^2 \right]$$

where  $\gamma$  is a small number and  $\ell$  is the beam radius.

We are exploring, as one possible coupling mechanism, the non-uniform plasma resonances discussed in the previous section. These resonances set up the high-order radial field variations required to excite transverse velocity beam waves. The resonances themselves may be excited by electrodes which are located entirely outside the beam-plasma region. (See Fig. 8.)

Many experiments related to this aspect have been conducted. From these experiments, it appears that the core resonances in a plasma are strongly excited by an external circuit. The depth of the absorption is well illustrated in Fig. 7, which shows oscilloscope traces of resonant dips in reflected power as viewed on a strip line excited at a frequency of 400 Mc/sec. Each trace is for the indicated ratio of wave frequency to cyclotron frequency;

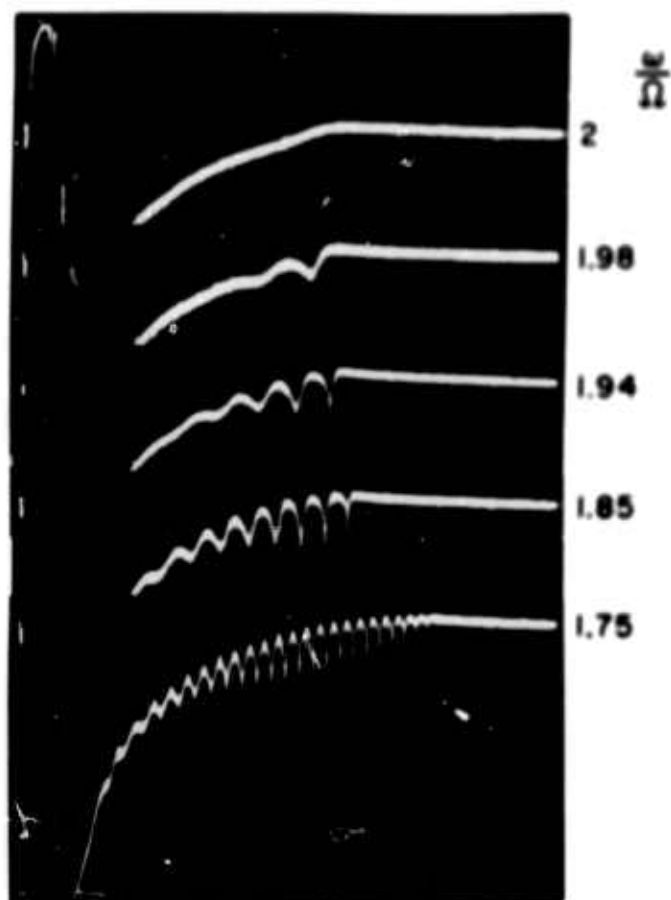


FIG. 7 Experimentally observed radial electron plasma wave resonances in the core of a cylindrical plasma column for different magnetic field strengths, observed in reflection in a neon afterglow plasma, 0.02 torr,  $f = 400$  Mc/sec, time scale 0.2 msec/div. Note depth of resonant structure.

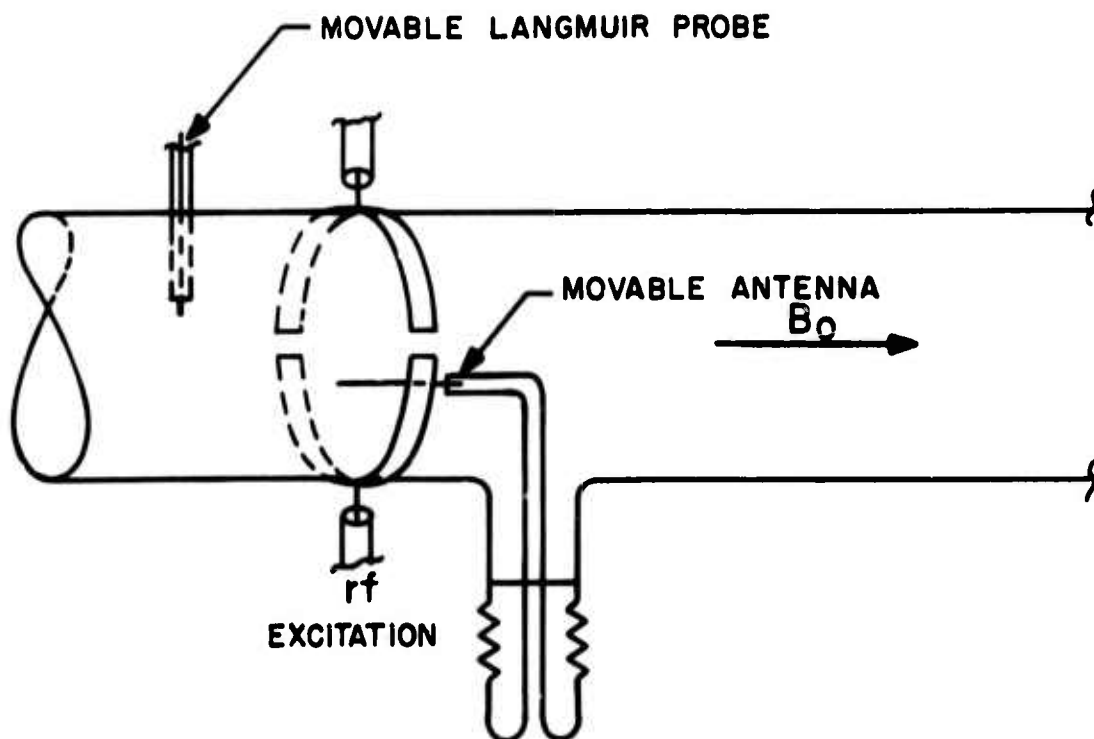


FIG. 8 Experimental apparatus showing method of excitation as well as method of internal probing of radial resonances on a plasma column in magnetic field. The rf excitation at 1175 Mc/sec is made on a capacitive type system employing striplines fed out of phase. A simple coaxial cable with the center conductor bared for one inch serves as the probe inside the dc discharge.



all traces in the vicinity of the second harmonic of the cyclotron frequency, as predicted by the dispersion relation of Bernstein<sup>12</sup> from longitudinal waves propagating across the magnetic field.

#### IV. WORK PERFORMED DURING REPORT PERIOD

##### A. Diamagnetic Measurements

In the last quarterly report, two methods for obtaining a measure of the perpendicular or azimuthal motion of an electron beam were discussed. The first method employs an electrostatic probe with two electrodes which are oriented so that the exposed surfaces face in opposite directions. The probe is placed in the beam and oriented with the planes of the exposed surfaces normal to the azimuthal direction and facing in opposite directions. A differential measurement of the probe signals is directly proportional to the azimuthal particle flux (Figs. 15 and 16 of Quarterly Report No. 6). This method is useful for obtaining an indication of the local azimuthal motion of an electron beam, provided that the probe is small enough not to disturb the beam and that the two electrodes are mechanically symmetrical. An absolute measurement is further complicated by secondary emission effects at the exposed metallic surfaces; these must be included in an analysis.

An alternative approach to the problem is to utilize the diamagnetic properties of the electron beam in a magnetic field. This method provides an integrated or average measurement of the azimuthal velocity over the beam cross section. The magnetic polarization due to electron motion is given by

$$\underline{M} = \frac{1}{\mu_0} \underline{B} - \underline{H}_0 \quad (7)$$

where  $\underline{H}_0$  is the magnetic field intensity in the absence of the beam. The polarization is given by the product of particle density and diamagnetic moment,

$$M = \frac{\frac{1}{2} m V_{\perp}^2}{B_0} n(r) \quad (8)$$

Here,  $V_{\perp}$  is the transverse velocity and  $B_0 = \mu_0 H_0$ . The reduction in the axial flux density  $\delta B$  is obtained from Eqs. (7) and (8) and is

$$\delta B = - \frac{\frac{1}{2} m V_{\perp}^2}{B_0} \mu_0 n(r) \quad (9)$$

where  $\delta B = B - B_0$ .

The change in magnetic flux is

$$\delta\phi = \int_A \delta \underline{B} \cdot d\underline{A} = - \frac{\pi m V_{\perp}^2}{B_0} \omega_0 \int_0^R n(r) r dr \quad (10)$$

where  $A$  is the cross-sectional area of the beam. The total beam current  $I$  is obtained by integrating the axial current density across the beam, i.e.,

$$I = \int_A \underline{J} \cdot d\underline{A} = - 2 \pi e V_{\parallel} \int_0^R n(r) r dr \quad (11)$$

where  $V_{\parallel}$  is the axial velocity of the beam electrons.

Combining (10) and (11) yields

$$\delta\phi = \left[ \frac{\omega_0 V_0}{2\Omega_c} \frac{\left(\frac{V_{\perp}}{V_0}\right)^2}{\left[1 - \left(\frac{V_{\perp}}{V_0}\right)^2\right]^{1/2}} \right] I \quad (12)$$

Here,  $\Omega_c$  is the electron-cyclotron frequency and  $V_0 = (V_{\parallel}^2 + V_{\perp}^2)^{1/2}$  is the speed of the electrons along their helical trajectory.

Experiments have been performed which used the above effect to measure the transverse energy. The electron gun consisted of a 3/8 inch cylindrical thermionic cathode, a planar grid, and a planar anode with a hole in it. The grid was used to gate the beam on and off at a 1000 Hz rate while the anode was kept at a constant potential with respect to the cathode. In this way, the beam current could be varied but the energy remained fixed. The electron gun was aimed into a region of increasing magnetic field at the end of a uniform solenoid and at an angle of  $30^\circ$  with respect to the symmetry axis. At the opposite end of the solenoid was a collector biased to collect the beam and any secondary electrons. A measurement of the cathode, grid and anode currents indicated that the ionization of background neutral gas (at a pressure  $\sim 2 \times 10^{-6}$  torr) was negligible and that the collector current was due entirely to beam electrons.

The fluctuating beam current resulted in a time varying magnetic flux whose effect was measured by passing the beam through a pickup coil.

The perpendicular velocity was then calculated from the proportionality constant of Eq. (12). The electrostatically shielded pickup coil consisted of approximately 2000 turns of No. 44 wire and had a radius of 1.75 inches and a length of 1.75 inches. The coil was placed coaxially with and well inside the solenoid where the magnetic field was uniform. The experimental arrangement is shown in Fig. 9. The signal obtained from the pickup coil was fed into a phase-sensitive amplifier together with a reference signal. The output of the amplifier was then used to drive the y-axis of a chart recorder. The average collector current was applied to the x-axis of the recorder. Since the beam was gated on and off, the average current was one half the peak value. Prior to the beam measurements, the system was calibrated by applying a square wave through a 1 M $\Omega$  resistor to the main solenoid. In this way the output of the lock-in amplifier was determined to be 1.75 mV per  $\mu$ gauss of fluctuating magnetic field.

Equation (12) indicates that the diamagnetic flux for a given collector current is directly proportional to the beam velocity  $V_0$  and varies inversely with the applied magnetic field. The results of a typical measurement in which the magnetic field was varied are shown in Fig. 10. As the applied magnetic field was increased, the diamagnetic flux decreased. The comparison of the measurement with theory is shown in Fig. 11, where the percentage of final beam energy in the transverse plane is plotted vs the axial magnetic field. Theoretical curves for both 30 $^\circ$  and 35 $^\circ$  injection angles are included because the mechanical angle that the electron gun makes with the symmetry axis may differ slightly from the injection angle. This discrepancy is due to the fact that the converging magnetic field at the entrance to the solenoid has both radial and axial components, and part of the gun assembly is off the axis.

The results of varying the total beam energy at a constant magnetic field are shown in Figs. 12 and 13. As the beam energy was increased, the diamagnetic flux also increased in approximately the expected manner. Additional measurements were made at constant beam energy and magnetic field, but with a varying distance from the electron gun to the entrance of the solenoid. As the gun was moved away from the entrance toward a region of weaker field, the percentage of transverse energy increased, in agreement with the adiabatic theory. The results of this measurement are shown in Fig. 14, together with a theoretical curve for 30 $^\circ$  injection which was derived from the known axial variation of magnetic field with distance.

#### B. Noise Emission from a Transverse Energy Beam

We have measured the noise radiated by an electron beam with transverse energy in a magnetic field. The output of a small dipole antenna placed close to the beam was fed into a high-gain superheterodyne receiver with a swept-frequency local oscillator. The detected output of the receiver was used to drive the y-axis of a chart recorder and the x-axis was synchronized with the local-oscillator scan. The spectrum could also be displayed on an oscilloscope. The transverse energy beam was obtained from a planar electron gun placed at an angle with respect to the solenoid axis, as described in the previous section.

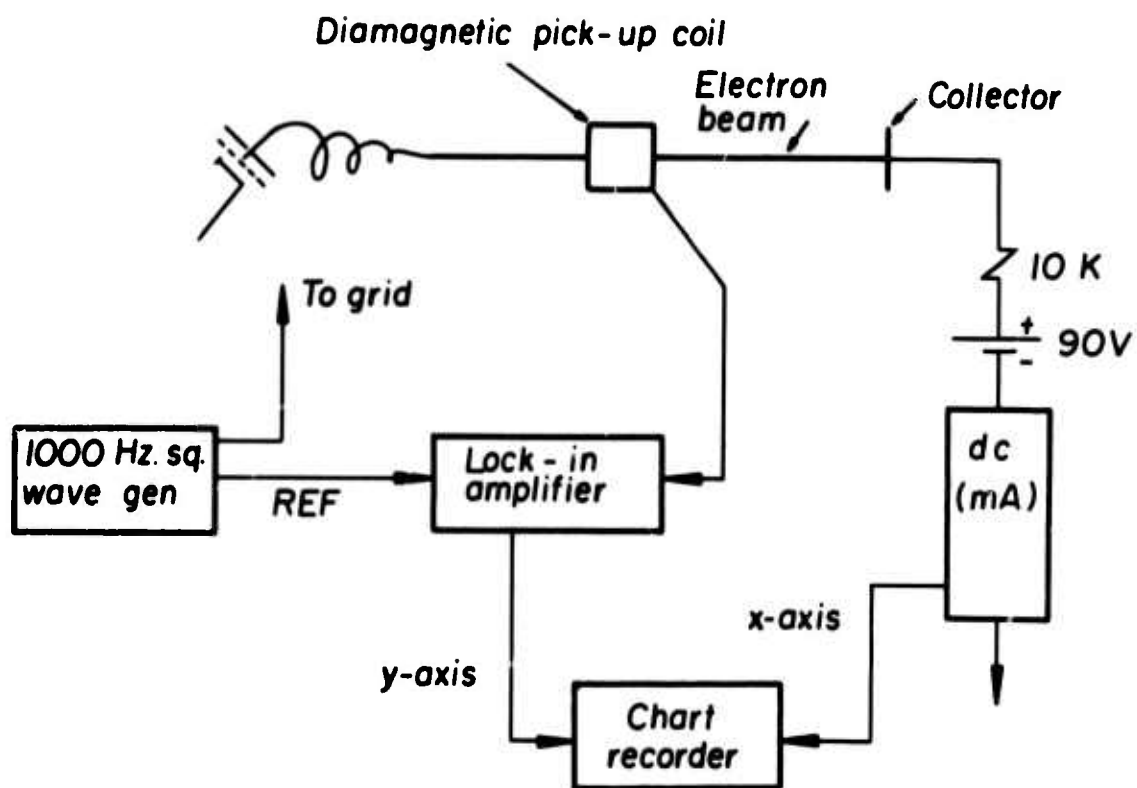


FIG. 9 Experimental arrangement for measuring the diamagnetism of an electron beam.

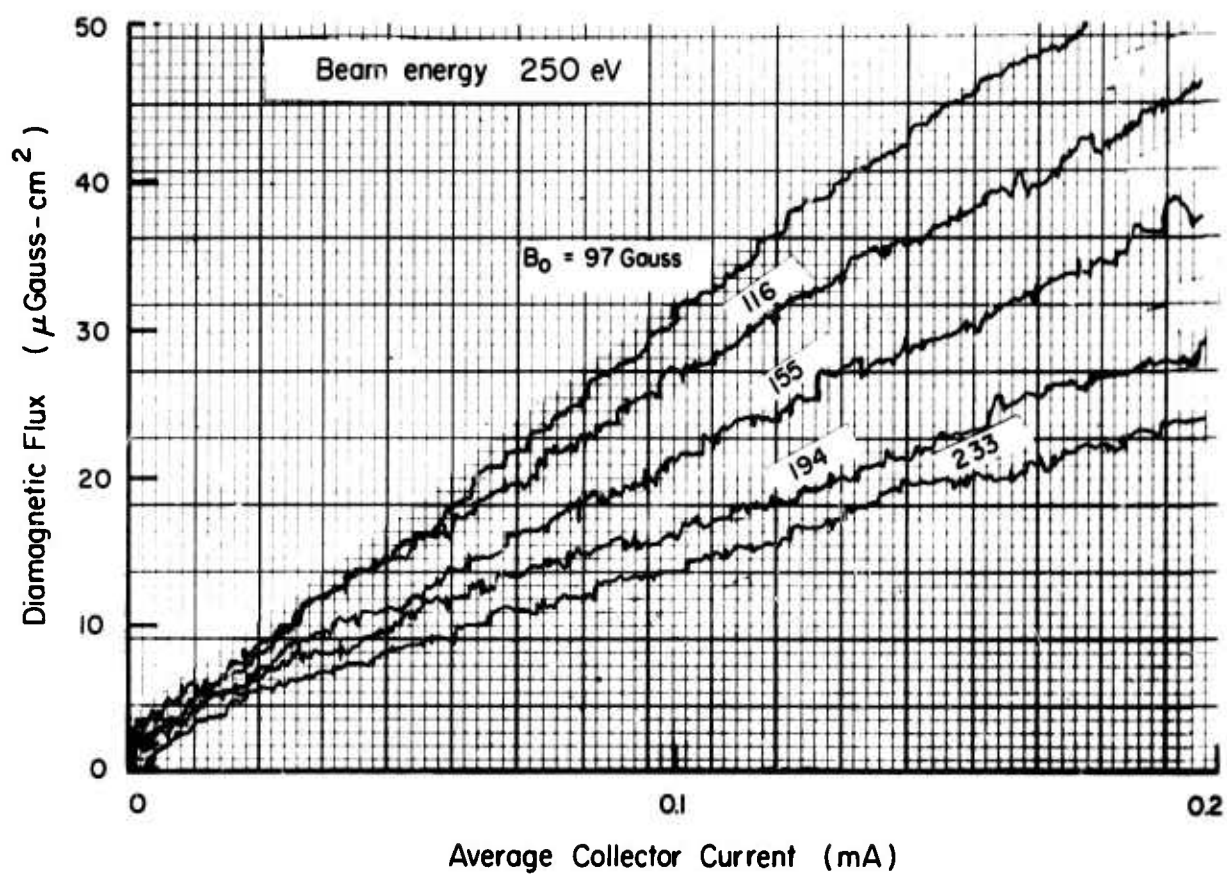


FIG. 10 Variation of diamagnetic flux with beam current for different magnetic fields with a fixed beam energy.

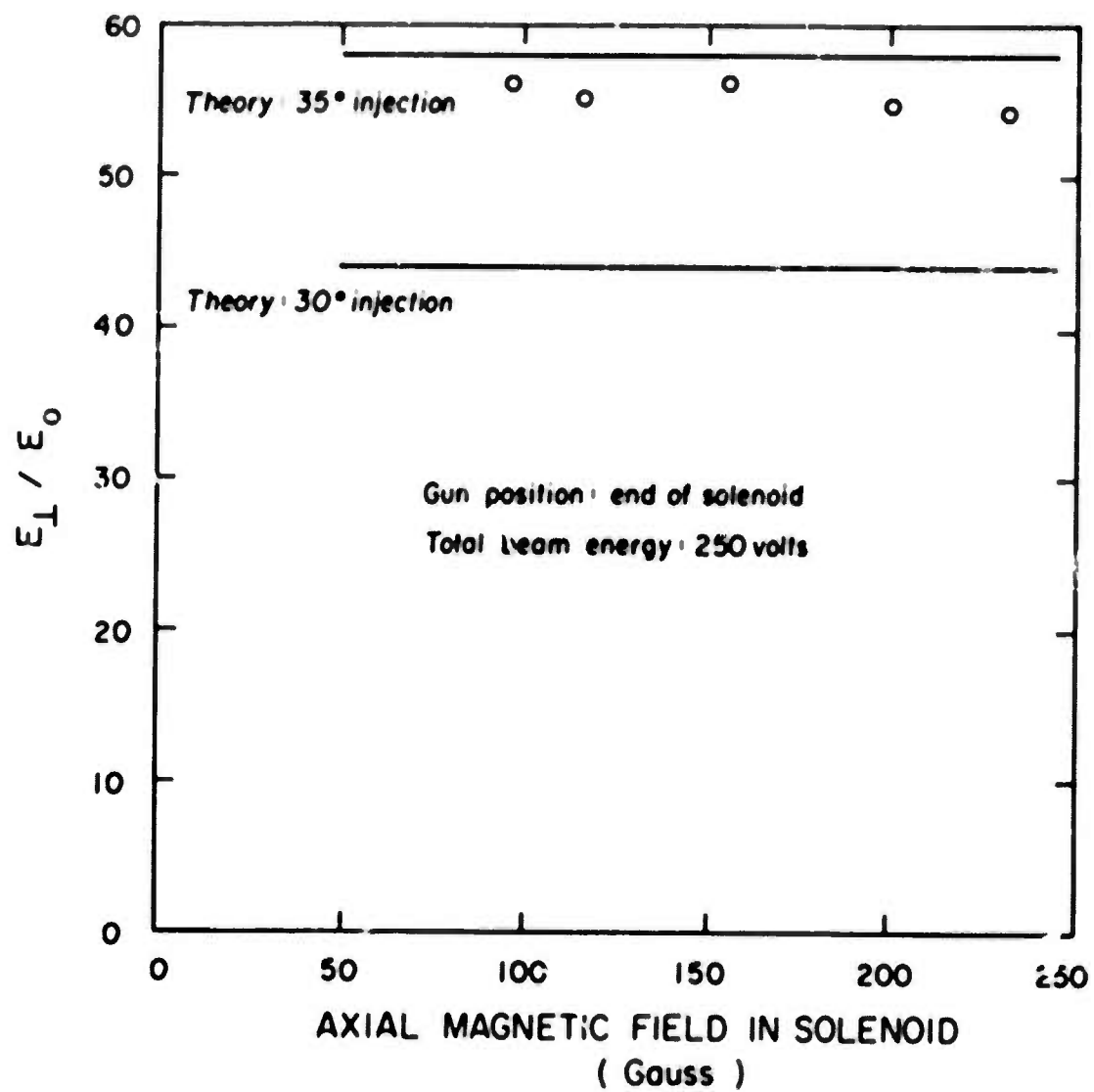


FIG. 11 Percentage of final beam energy in the transverse plane as a function of axial magnetic field.

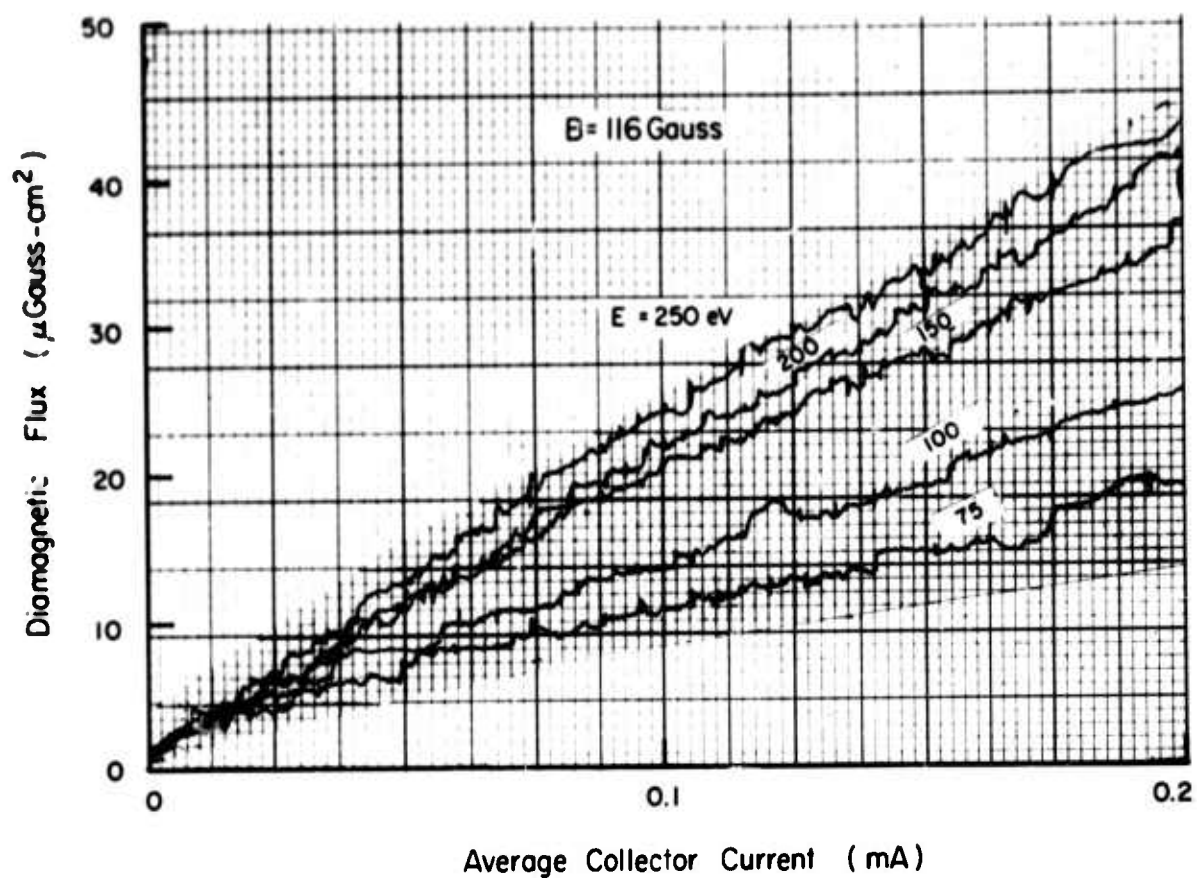


FIG. 12 Variation of diamagnetic flux with beam current for different beam currents at a fixed magnetic field.

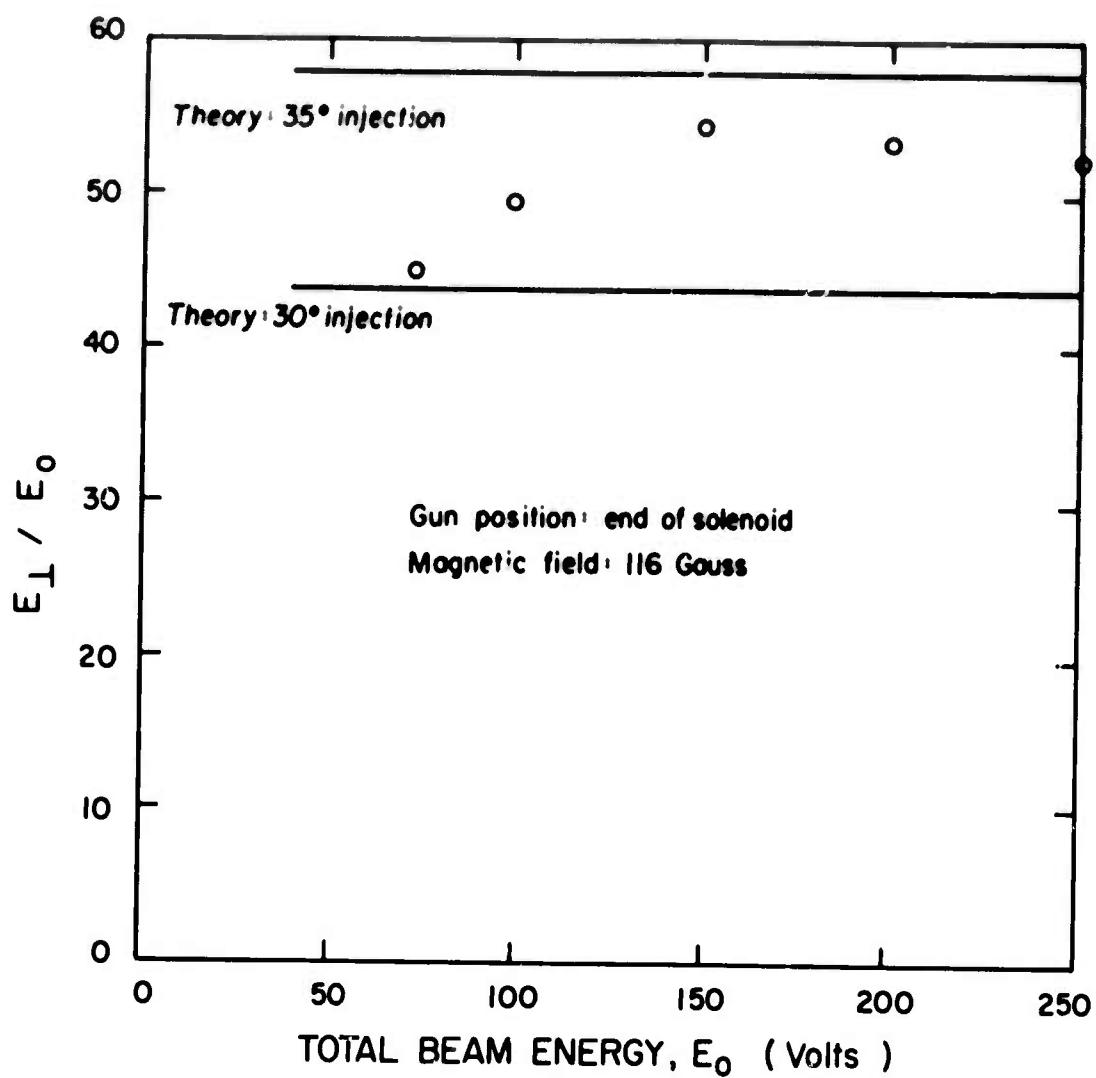


FIG. 13 Percentage of final beam energy in the transverse plane as a function of the total energy in the electron beam.



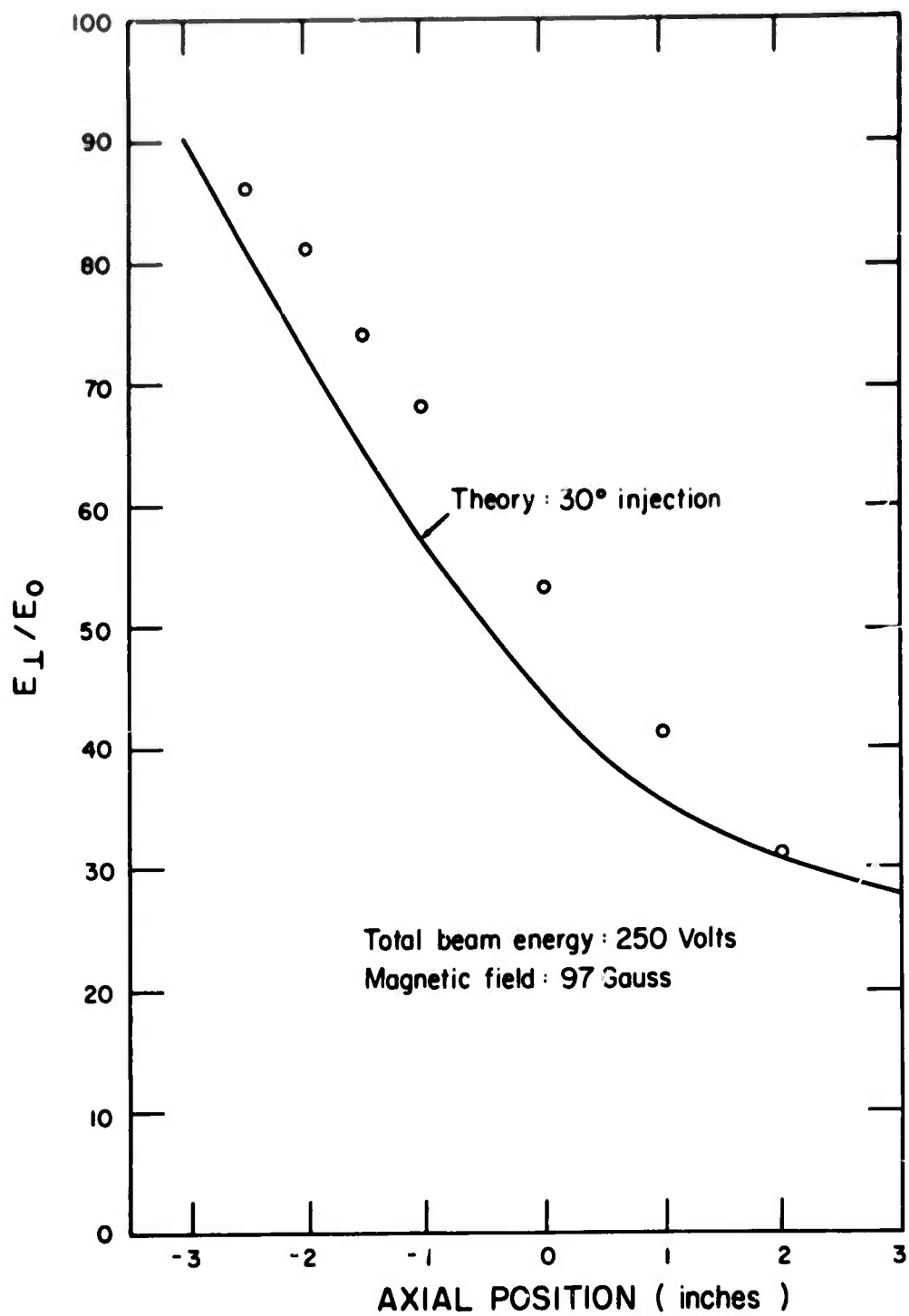


FIG. 14 Percentage of axial beam energy in the transverse planes as a function of the axial position of the gun. The axial position origin is at the end of the solenoid.

The output of the receiver showed discrete noise peaks at the electron-cyclotron frequency and its first three harmonics. The results of a sequence of observations in which the applied axial magnetic field was varied are shown in Fig. 15. The data points show the frequency and axial magnetic field at which noise emission was observed. The electron beam energy was 300 eV and the current was 0.86 mA. The peak noise power radiated at the fundamental was determined to be  $14.8 \times 10^{-9}$  W/MHz by comparison with a calibrated noise source. The width at half maximum was 4 MHz at a cyclotron frequency of 162 MHz.

The noise peaks were observed to shift away from the cyclotron frequency towards higher frequency when a neutral gas was allowed to enter the vacuum chamber. The results of a sequence of observations as the background pressure of helium was varied are shown in Fig. 16. As the pressure increased above  $10^{-4}$  torr, the frequency of the noise peaks increased sharply. This behavior suggests that the emission may follow the hybrid frequency  $f = (f_c^2 + f_p^2)^{1/2}$ , where  $f_c$  is the cyclotron frequency and  $f_p$  is the plasma frequency of the beam-produced plasma.

### C. Modulated-Beam Experiment

In the previous report we described measurements of the phase of waves excited in the plasma by a density-modulated beam as a function of beam voltage and for various magnetic fields. These results were not consistent with a model in which the axial wavelength of the plasma waves is equal to the separation between charge maxima on the beam, chiefly because this model does not predict an observed change of axial wavelength with magnetic field. Recently, Gruber (private communication) has suggested that the plasma waves may be excited by a transverse energy beam mode near the second harmonic. The approximate dispersion characteristics of the mode of frequency  $\omega$  are

$$2\omega_c - \omega = k_{\parallel} v_{\parallel} \quad (13)$$

where  $\omega_c$  is the cyclotron frequency,  $k_{\parallel}$  is the axial wave number, and  $v_{\parallel}$  is the axial velocity of the beam. An alternate possibility is that the plasma waves beat with this beam mode (beating of the plasma waves with a relatively long wavelength wave is required to account for the observed radial amplitude variations described in earlier reports).

In either case, the beam voltage  $V$  determines the number of axial wavelengths between the probe and a fixed phase point on the beam. If this point is a distance  $L$  along the beam from the probe, the number of wavelengths is

$$n = \frac{Lk_{\parallel}}{2\pi} = \frac{L(2\omega_c - \omega)}{2\pi v_{\parallel}} = \sqrt{\frac{m}{2e}} \frac{L}{2\pi} (2\omega_c - \omega) \cdot \frac{1}{\sqrt{V}}$$

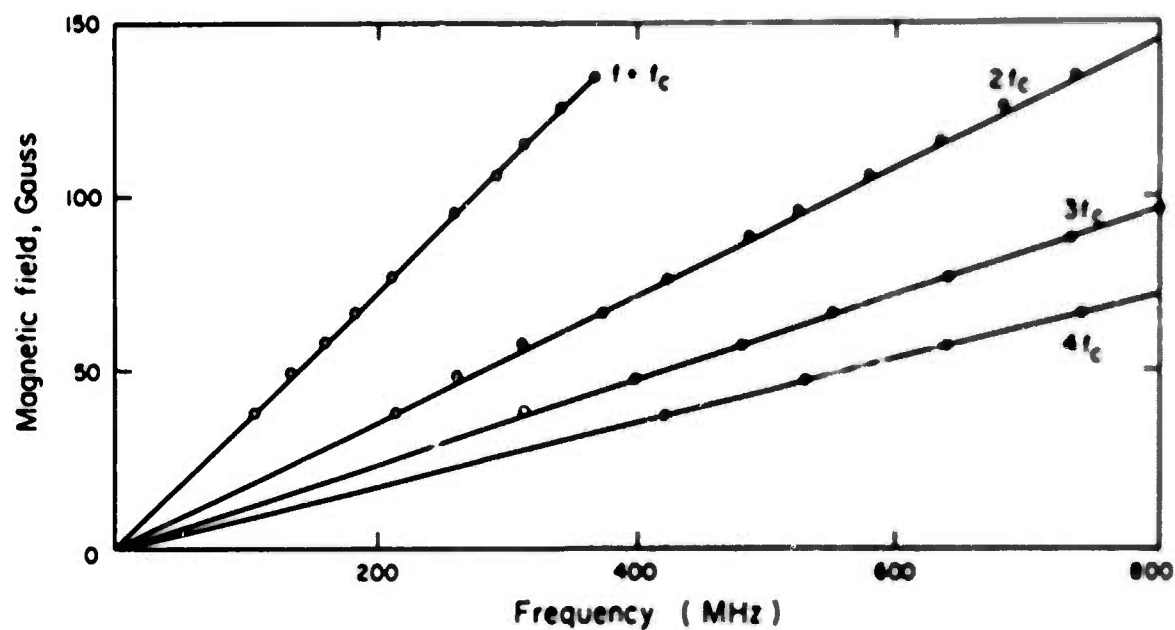


FIG. 15 Dependence of noise frequency radiated by transverse energy beam on axial magnetic field. Noise emission is at the fundamental cyclotron frequency ( $f_c$ ) and its noise harmonics.

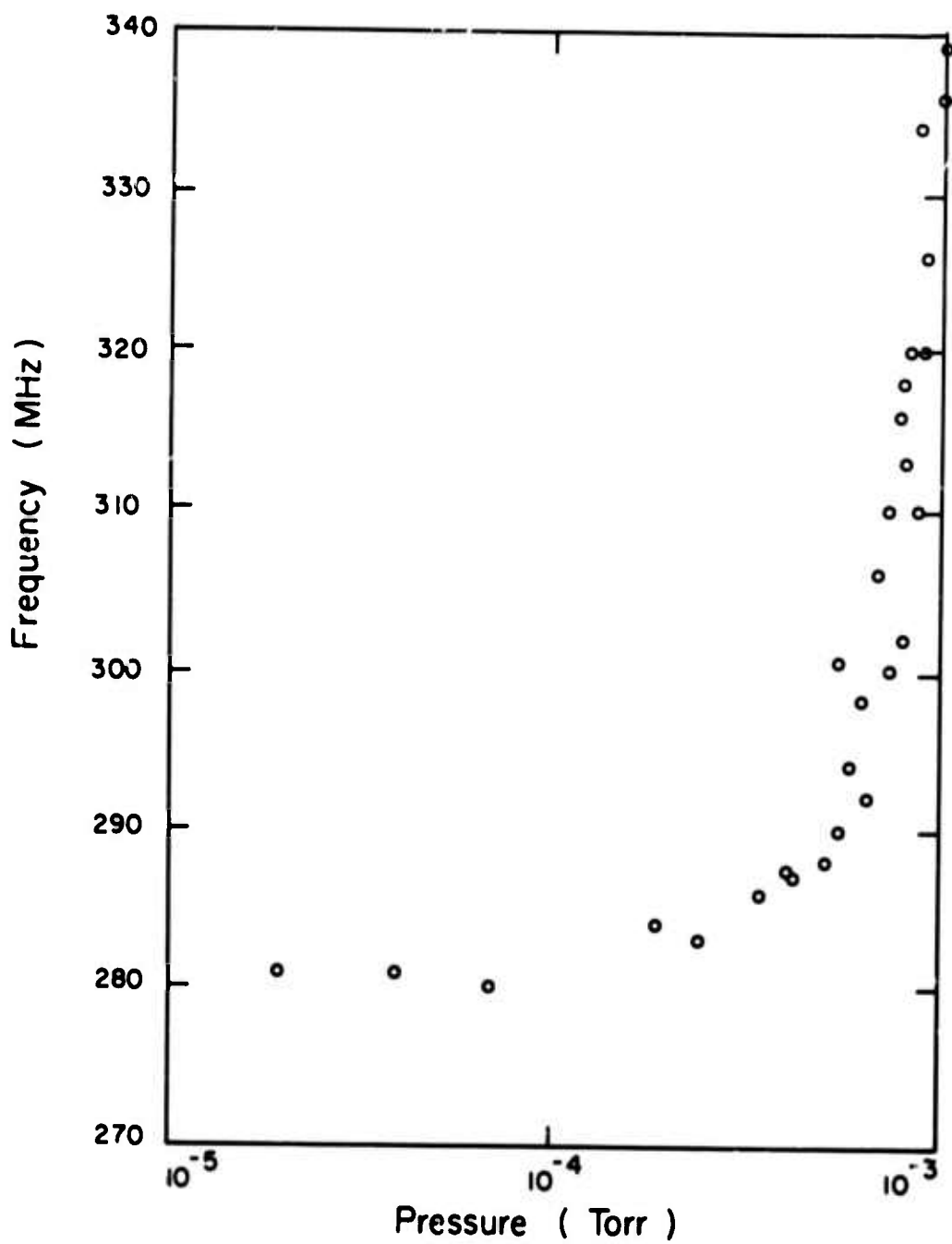


FIG. 16 Frequency of noise emitted near the cyclotron frequency as a function of helium pressure. The emitted frequency rises above the cyclotron frequency as the pressure increases.

where  $e$  and  $m$  are the charge and mass of the electron. This equation predicts that graphs of  $n$  against  $1/\sqrt{V}$  should be straight lines whose slopes are proportional to  $(2\omega_c - \omega)$ . Figure 17 shows  $n$  plotted against  $1/\sqrt{V}$  for several magnetic fields. (Note that there is no correlation between the number  $n$  at the different magnetic fields, because of radial phase variations with field.) The voltage  $V$  is the accelerating anode voltage, with 40 volts added to allow for the energy given to the electrons by the rf fields in the cavity which produces the beam modulation (this value gives the best straight lines in Fig. 17). The slopes of the lines are accurately proportional to  $(2\omega_c - \omega)$ . However, the length  $L$  derived from the slopes is 55 cm, which is considerably larger than the distance of either end of the system from the measuring probes. In spite of this discrepancy, the results suggest that the beam mode described by Eq. (13) plays a part in determining the radiation pattern. Although transverse energy is required for the existence of this mode on the beam, these experiments were carried out with the beam gun mounted coaxially with and immersed in the magnetic field and with no corkscrew magnetic fields. However, a certain amount of transverse energy will exist on the beam due to non-uniformities in the system.

## V. CONCLUSIONS

A system for measuring the transverse energy on a beam through its diamagnetism has been developed. The method was used to measure the transverse energy of a beam injected across the magnetic field lines. Analysis of data in the beam plasma interaction experiment has indicated the possible existence of a transverse energy beam mode in our experiments.

## VI. FUTURE PLANS

The angled injection beam, which has a large fraction of its energy in the transverse direction, will be used in a two-beam experiment and in beam-plasma interaction experiments. Attempts will be made to detect the transverse energy mode near the second harmonic on an electron beam in a vacuum.

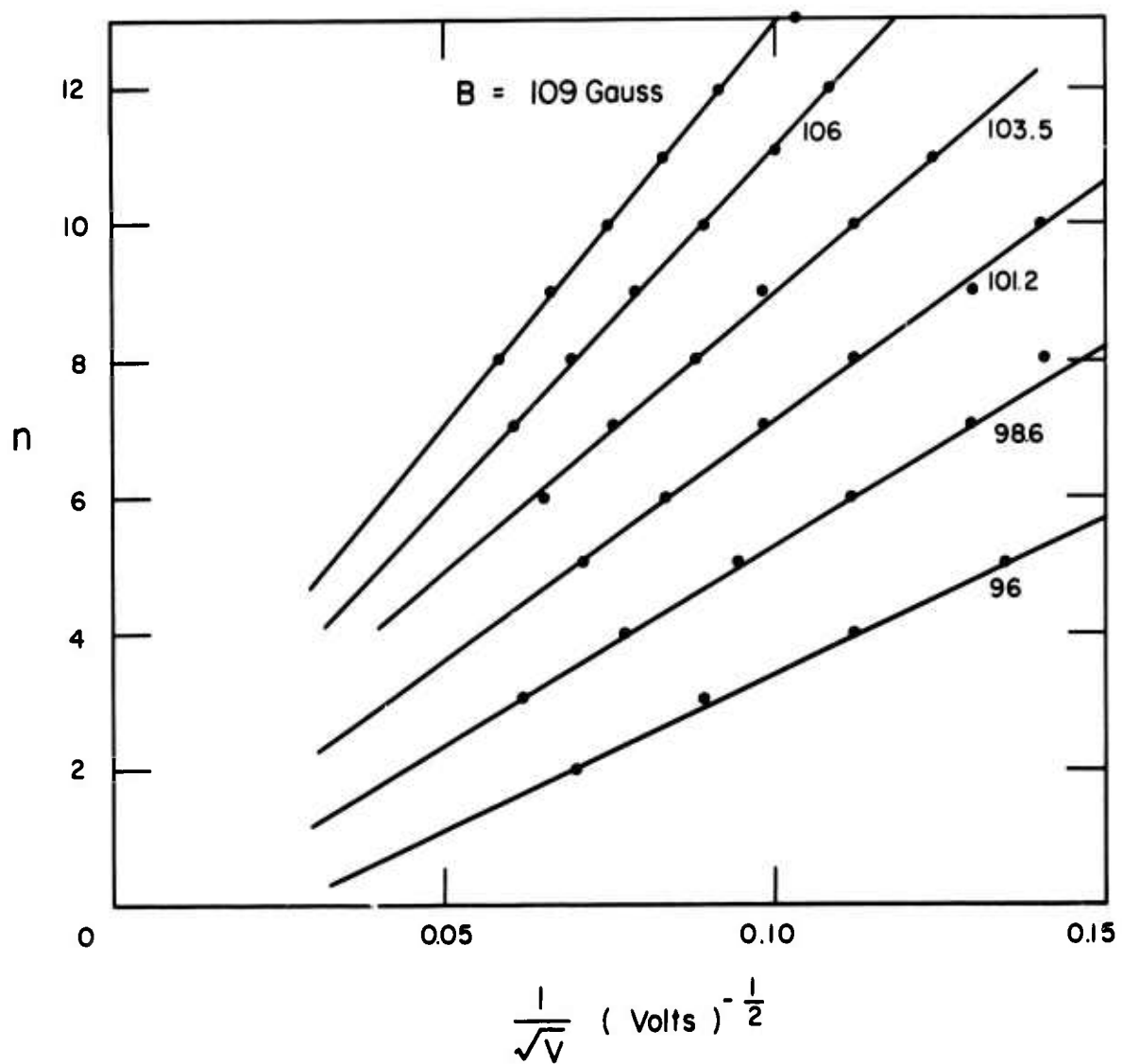


FIG. 17 Axial beam voltage  $V$  at which maxima, numbered  $n$ , are observed with a fixed probe in the plasma.

#### LITERATURE CITED

1. R. W. Gould and A. W. Trivelpiece, A New Mode of Wave Propagation on Electron Beams, Proceedings of the Symposium on Electronic Waveguides, (Polytechnic Press, Brooklyn, New York, 1958).
2. L. D. Smullin and P. Chorney, Propagation in Ion Loaded Waveguides, ibid.
3. P. L. Auer and S. Gruber, Bull. Am. Phys. Soc. II 9, 565 (1964).
4. S. Gruber, Bull. Am. Phys. Soc. II 10, 221 (1965).
5. A. Bers and S. Gruber, Appl. Phys. Letters 6, 27 (1965).
6. S. Gruber, M. W. Klein and P. L. Auer, Phys. Fluids 8, 1504 (1965).
7. A. Simon and M. N. Rosenbluth, Phys. Fluids 6, 1566 (1963).
8. J. Nickel, J. Parker and R. W. Gould, Phys. Fluids 7, 1489 (1964).
9. S. J. Buchsbaum and A. Hasegawa, Phys. Rev. Letters 12, 685 (1964).
10. H. J. Schmitt, G. Meltz and P. J. Freyheit, Phys. Rev. 139, A1432 (1965).
11. K. Mitani, H. Kubo and S. Tanaka, J. Phys. Soc. (Japan) 19, 221 (1964).
12. J. B. Bernstein, Phys. Rev. 109, 10 (1958).

Unclassified

Security Classification

| DOCUMENT CONTROL DATA - R&D   |  |   |
|---|--|---|
| (Security classification of title, body of abstract and indexing annotation must be entered when the overall report is classified)  |  |   |
| 1 ORIGINATING ACTIVITY (Corporate author)<br>SPERRY RAND RESEARCH CENTER<br>SUDBURY, MASSACHUSETTS 01776  |  | 2a REPORT SECURITY CLASSIFICATION<br>Unclassified |
|   |  | 2b GROUP<br>-----                                 |
| 3 REPORT TITLE<br>INVESTIGATION OF HIGH-POWER BEAM-PLASMA INTERACTIONS  |  |   |
| 4 DESCRIPTIVE NOTES (Type of report and inclusive dates)<br>Seventh Quarterly Report: 15 June 1967 - 14 Sept. 1967  |  |   |
| 5 AUTHOR(S) (Last name, first name, initial)<br>Ewald, Harry; Lustig, Claude; Morse, David L.   |  |   |
| 6 REPORT DATE<br>December 1967  | 7a TOTAL NO. OF PAGES<br>31  | 7b NO. OF REFS<br>12                              |
| 8a CONTRACT OR GRANT NO<br>DA28-043-AMC-01821(E)  | 9a ORIGINATOR'S REPORT NUMBER(S)<br>SRRC-CR-67-57  |   |
| b PROJECT NO<br>7900.21.243.40.01   |  |   |
| c ARPA Order No. 695  | 9b OTHER REPORT NO(S) (Any other numbers that may be assigned this report)<br>ECOM-01821-7                         |   |
| 10 AVAILABILITY LIMITATION NOTICES<br>Each transmittal of this document outside the Department of Defense must have prior approval of CGS, U.S. Army Electronics Command, Fort Monmouth, N.J., 07703<br>Attn: AMSEL-KL-TG   |  |   |
| 11 SUPPLEMENTARY NOTES<br>Advanced Research Projects Agency<br>ARPA Order No. 695   | 12 SPONSORING MILITARY ACTIVITY<br>U.S. Army Electronics Command<br>Fort Monmouth, N.J. 07703<br>Attn: AMSEL-KL-TG |   |
| 13 ABSTRACT<br><p>This research is directed toward the investigation of high-power beam plasma interactions, with specific investigation of the transverse velocity beam modes called for.</p> <p>A system for measuring the transverse energy of an electron beam through its diamagnetism has been developed and used to measure the transverse energy of a beam injected across magnetic field lines. In investigations of the noise emission from a transverse energy beam, discrete noise peaks, which shifted toward higher frequencies when a neutral gas was allowed to enter the vacuum chamber, occurred at the electron-cyclotron frequency and its first three harmonics. Experiments in helium indicate that the emission may be described by a hybrid frequency relationship. Analysis of the data from beam plasma interaction experiments has indicated the possible existence of a transverse energy beam mode on our experiments.</p> <p>This research is part of PROJECT DEFENDER, sponsored by the advanced Research Project Agency, Department of Defense, and administered by the U.S. Army Electronics Command under Contract No. DA28-043-AMC-01821(E).</p> |  |   |

DD FORM 1473

Unclassified

Security Classification



| 14<br>KEY WORDS   | LINK A |    | LINK B |    | LINK C |    |
|---|--------|----|--------|----|--------|----|
|   | ROLE   | WT | ROLE   | WT | ROLE   | WT |
| Beam-plasma interactions<br>Microwave devices<br>Electron beams<br>Electrostatic wave resonance<br>Wave coupling<br>Plasma column resonance |        |    |        |    |        |    |

**INSTRUCTIONS**

**1. ORIGINATING ACTIVITY:** Enter the name and address of the contractor, subcontractor, grantee, Department of Defense activity or other organization (corporate author) issuing the report.

**2a. REPORT SECURITY CLASSIFICATION:** Enter the overall security classification of the report. Indicate whether "Restricted Data" is included. Marking is to be in accordance with appropriate security regulations.

**2b. GROUP:** Automatic downgrading is specified in DoD Directive 5200.10 and Armed Forces Industrial Manual. Enter the group number. Also, when applicable, show that optional markings have been used for Group 3 and Group 4 as authorized.

**3. REPORT TITLE:** Enter the complete report title in all capital letters. Titles in all cases should be unclassified. If a meaningful title cannot be selected without classification, show title classification in all capitals in parenthesis immediately following the title.

**4. DESCRIPTIVE NOTES:** If appropriate, enter the type of report, e.g., interim, progress, summary, annual, or final. Give the inclusive dates when a specific reporting period is covered.

**5. AUTHOR(S):** Enter the name(s) of author(s) as shown on or in the report. Enter last name, first name, middle initial. If military, show rank and branch of service. The name of the principal author is an absolute minimum requirement.

**6. REPORT DATE:** Enter the date of the report as day, month, year; or month, year. If more than one date appears on the report, use date of publication.

**7a. TOTAL NUMBER OF PAGES:** The total page count should follow normal pagination procedures, i.e., enter the number of pages containing information.

**7b. NUMBER OF REFERENCES:** Enter the total number of references cited in the report.

**8a. CONTRACT OR GRANT NUMBER:** If appropriate, enter the applicable number of the contract or grant under which the report was written.

**8b, 8c, & 8d. PROJECT NUMBER:** Enter the appropriate military department identification, such as project number, subproject number, system numbers, task number, etc.

**9a. ORIGINATOR'S REPORT NUMBER(S):** Enter the official report number by which the document will be identified and controlled by the originating activity. This number must be unique to this report.

**9b. OTHER REPORT NUMBER(S):** If the report has been assigned any other report numbers (either by the originator or by the sponsor), also enter this number(s).

**10. AVAILABILITY/LIMITATION NOTICES:** Enter any limitations on further dissemination of the report, other than those imposed by security classification, using standard statements such as:

- (1) "Qualified requesters may obtain copies of this report from DDC."
- (2) "Foreign announcement and dissemination of this report by DDC is not authorized."
- (3) "U. S. Government agencies may obtain copies of this report directly from DDC. Other qualified DDC users shall request through \_\_\_\_\_."
- (4) "U. S. military agencies may obtain copies of this report directly from DDC. Other qualified users shall request through \_\_\_\_\_."
- (5) "All distribution of this report is controlled. Qualified DDC users shall request through \_\_\_\_\_."

If the report has been furnished to the Office of Technical Services, Department of Commerce, for sale to the public, indicate this fact and enter the price, if known.

**11. SUPPLEMENTARY NOTES:** Use for additional explanatory notes.

**12. SPONSORING MILITARY ACTIVITY:** Enter the name of the departmental project office or laboratory sponsoring (paying for) the research and development. Include address.

**13. ABSTRACT:** Enter an abstract giving a brief and factual summary of the document indicative of the report, even though it may also appear elsewhere in the body of the technical report. If additional space is required, a continuation sheet shall be attached.

It is highly desirable that the abstract of classified reports be unclassified. Each paragraph of the abstract shall end with an indication of the military security classification of the information in the paragraph, represented as (TS), (S), (C), or (U).

There is no limitation on the length of the abstract. However, the suggested length is from 150 to 225 words.

**14. KEY WORDS:** Key words are technically meaningful terms or short phrases that characterize a report and may be used as index entries for cataloging the report. Key words must be selected so that no security classification is required. Identifiers, such as equipment model designation, trade name, military project code name, geographic location, may be used as key words but will be followed by an indication of technical context. The assignment of links, rules, and weights is optional.